Conference on Modelling Fluid Flow (CMFF'25)
The 19th International Conference on Fluid Flow Technologies
Budapest, Hungary, August 26 - August 29, 2025

EXPERIMENTAL AND NUMERICAL INVESTIGATIONS OF NOZZLE SPACING EFFECTS ON FLOW CHARACTERISTICS OF TRIPLE RECTANGULAR FREE JETS

Koichi HAYASHIDA[1], Takahiro KIWATA[2], Peter OSHKAI[3]

[1] Corresponding Author. Graduate School of Natural Science and Technology, Kanazawa University. Kakuma-machi, Kanazawa-shi, Ishikawa, Japan. Tel.: +81 778 62 8309, E-mail: hayashida@fukui-nct.ac.jp
[2] School of Mechanical Engineering, Kanazawa University. E-mail: kiwata@se.kanazawa-u.ac.jp
[3] Department of Mechanical Engineering, University of Victoria. E-mail: poshkai@uvic.ca

ABSTRACT

The effect of nozzle spacing on the flow characteristics of triple rectangular free jets was studied experimentally and numerically. The nozzle spacing ratio S/d_e, where d_e is the equivalent diameter of a rectangular nozzle with an aspect ratio of 2, was varied from 2.06 to 4.13. The Reynolds number based on the nozzle exit velocity and the equivalent diameter was 1.5×10^4. The mean and fluctuating velocities were measured using a constant-temperature hot-wire anemometer with an X-type probe. Three-dimensional numerical simulations of triple rectangular free jets were also performed using Open FOAM 5.0, and the numerical results depicted the vortical structures in the jets. Triple rectangular free jets with a small nozzle spacing ratio, specifically S/d_e = 2.06, merge upstream. The mean velocity and the turbulent kinetic energy near the jet centerline become higher than those with a large nozzle spacing ratio. An axis-switching phenomenon occurs after the jets merge, and the whole cross-sectional shape of the triple rectangular free jets changes to an elliptical jet with a major axis in the z-direction. Farther downstream, the elliptical jet becomes round.

Keywords: flow measurement, hot-wire anemometry, nozzle spacing, OpenFOAM, rectangular jet, triple jets

NOMENCLATURE

B	[m]	width of rectangular nozzle
C	[m]	height of rectangular nozzle
C_s	[-]	Smagorinsky constant
d	[m]	diameter of circular nozzle
d_e	[m]	equivalent diameter of non-circular nozzle
k	[m^2/s^2]	turbulent kinetic energy
Q	[-]	second invariant iso-surface of velocity gradient tensor
Re	[-]	Reynolds number
S	[m]	nozzle spacing between the center of nozzles
u	[m/s]	x-axial velocity (streamwise velocity)
$\overline{u}$	[m/s]	mean x-axial velocity (streamwise mean velocity)
u'_{rms}	[m/s]	root-mean-square value of x-axial velocity fluctuation
$\overline{u}_{0cl}$	[m/s]	nozzle exit mean x-axial velocity at the center of nozzle
v	[m/s]	y-axial velocity
w	[m/s]	z-axial velocity
x	[m]	x-axial coordinate
x_c	[m]	potential core length
y	[m]	y-axial coordinate
z	[m]	z-axial coordinate
ν	[m^2/s]	kinematic viscosity

Subscripts

cl	on the jet centerline
cl,mid	on the jet centerline of the middle jet
cl,side	on the jet centerline of the side jet
sym	on the jet symmetry-line

1. INTRODUCTION

Multiple jets issuing from two or more nozzles are used in various applications, such as aircraft combustors, air ventilation systems, and chip removal systems in machine tools. The flow structures of twin jets, which issue from two nozzles arranged in parallel, have been reported by several researchers [1-3]. For example, the effects of nozzle spacing on the flow characteristics of twin circular jets were investigated by Okamoto et al. [1] and Laban et al. [2]. They reported that, for a small spacing ratio S/d, the twin circular jets merged at the

upstream side, and the streamwise mean velocity on the jet centerline increased due to the suppression of the entrainment with ambient flow in the inner shear layer.

A single non-circular jet provides higher mixing capabilities with the ambient fluid than those of a single circular jet due to the three-dimensional deformation of the vortex rings in the free shear layer. Therefore, the flow structure of multiple non-circular jets is expected to be more complex than that of multiple circular jets. Hayashida and Kiwata [4] experimentally studied the effects of the nozzle orientation and nozzle spacing on the flow characteristics of twin rectangular free jets with a nozzle aspect ratio of 2. They showed that, for a small nozzle spacing, the mean and fluctuating velocities of twin rectangular free jets become larger, after the combined point (CP) on the jet symmetry line, than those of a single circular jet. However, the nozzle orientation has little effect on the mean and fluctuating velocities.

Figure 1 shows a schematic diagram of the *x*-*y* cross-section of the flow field of the triple rectangular free jets described in the present paper. The flow field of the triple jets, which are lined up in a row, is divided into the converging, the merging, and the combined regions. The converging region ends at the plane corresponding to the merging point (MP), that is, $\overline{u}_{sym} \approx 0.015\overline{u}_{0cl}$. The combined region is formed downstream of the CP, where $\overline{u}_{cl,side} \approx \overline{u}_{sym}$. The region between these two regions is referred to as the merging region. The region between the middle jet and the side jets is defined as the inner mixing region, and the region between the side jets and the ambient fluid is defined as the outer mixing region. Thus, the shear layers in the outer mixing regions are defined as the outer shear layers. The shear layers in the inner mixing region are defined as the outside and inside inner shear layers, respectively. As shown in Fig. 1, the flow field of the triple jets is more complicated than that of the twin jets, because the middle jet is influenced by the adjacent jets. Morris et al. [5] investigated the effect of nozzle orientation on the flow characteristics of multiple non-circular jets with triple elliptic nozzles with an aspect ratio of 2, and a nozzle spacing of $4.1d_e$. They found that the triple elliptic jets with each nozzle oriented along the minor plane had a shorter potential core length and a closer MP location where the inner mixing region of the adjacent jets merge than the other orientations. However, they did not investigate the effect of nozzle spacing ratio.

The objective of the present research was to investigate the effect of nozzle spacing on the flow characteristics of triple rectangular free jets with each nozzle oriented along the major plane and having an aspect ratio of 2. This paper describes the distributions of velocity and turbulence intensity obtained experimentally using an X-type hot-wire probe, and large eddy simulation (LES) results obtained using the computational fluid dynamics (CFD) software OpenFOAM 5.0.

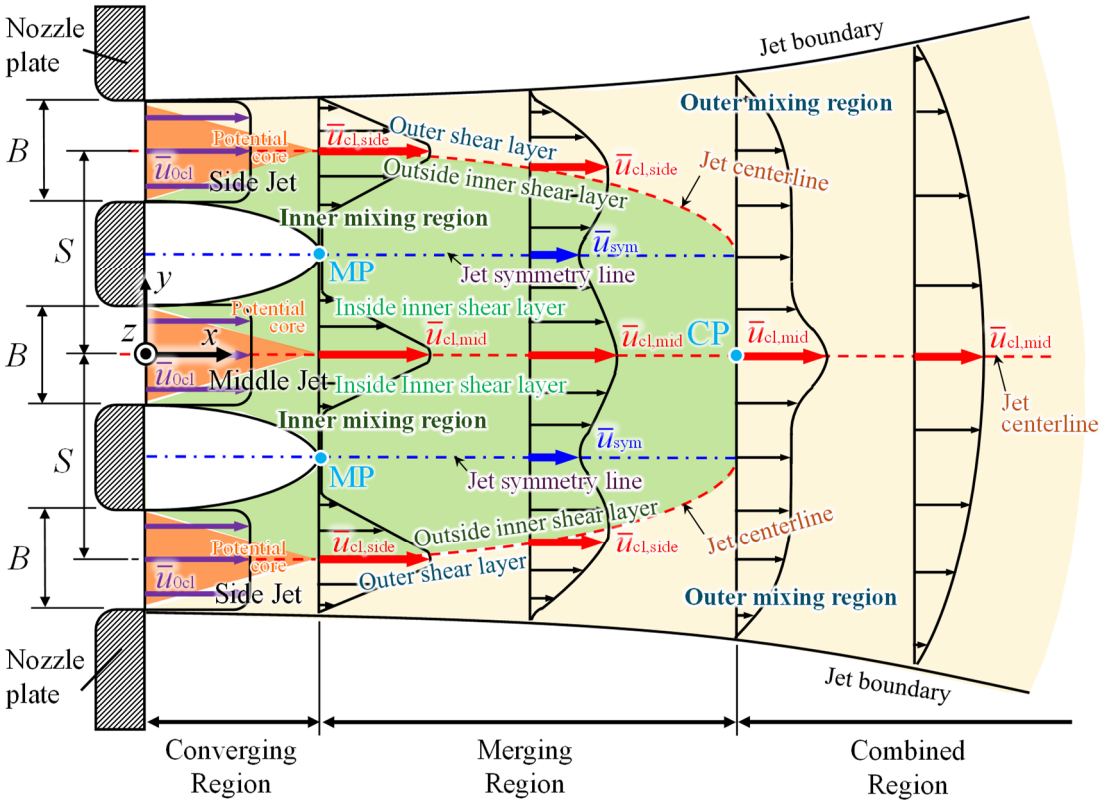

Figure 1. Schematic diagram of the flow field of triple rectangular free jets.

2. EXPERIMENTAL PROCEDURE AND NUMERICAL SETUP

2.1. Experimental apparatus and method

Figure 2 shows a schematic diagram of the experimental system [6]. Figure 3 shows a schematic diagram of an orifice plate with triple rectangular nozzles. The orifice plate was installed at the wind tunnel outlet to generate the rectangular free jets. The orifice plate was made of an acrylic resin 10 mm thick. Each rectangular nozzle had a height of $C = 10$ mm, a width of $B = 20$ mm, and a constriction formed by a circular shoulder with a radius $R = 4$ mm at the upstream edge of the orifice to prevent flow separation. The aspect ratio of the rectangular nozzle was $B/C = 2$, and the equivalent diameter of each nozzle was $d_e\,[= (4BC/\pi)^{1/2}] \approx 15.96$ mm. The nozzle spacing between the centers of the triple rectangular free jets was varied as $S = 33$ mm to 66 mm, specifically the four spacing ratios of $S/d_e = 2.06$ to 4.13. The nozzles were aligned with their major axes. The flow characteristics of a single rectangular free jet, a single circular free jet, and twin rectangular free jets were also investigated to compare with those of triple rectangular free jets. The results of the single rectangular free jet, twin rectangular free jet, and the single circular jet in the x-y cross-section on the major axis are referred to as "SingleMajor," "TwinMajor," and "SingleRound" configurations, respectively. The definition of the x, y, and z axes is shown in Figs. 1 and 2. The coordinate origin in the flow field of triple rectangular free jets was set to the center of the middle nozzle outlet. The flow direction was defined as x; the horizontal direction as y; the vertical direction as z; and velocity in each direction as u, v, and w, respectively.

The flow velocities were measured by an X-type hot-wire probe and constant-temperature hot-wire anemometers (CTA) with linearized output. The hot-wire probe could be moved three-dimensionally by a traverse unit. The output signals from the CTA were converted by a 16-bit analog/digital (A/D) converter at a sampling frequency of 6 kHz and 1.2×10^5 data points were recorded. The resulting digital signals were used to calculate the mean and the fluctuating velocities. Aleyasin and Tachie [3] found that, for Reynolds number $Re > 1.0 \times 10^4$, the velocity decay and the jet spread of twin circular jets are independent of the Reynolds number. Therefore, the Reynolds number was set to $Re = \bar{u}_{0cl}\, d_e/\nu = 1.5 \times 10^4$, where ν is the kinematic viscosity of air. The mean velocity at the center of the nozzle exit, that is, $x/d_e = 0.1875$, $y/d_e = 0$, and $z/d_e = 0$, was set to $\bar{u}_{0cl} \approx 14.2$ m/s. Further, the uncertainties of the mean velocity and the fluctuating velocity components measured using an X-type hot-wire probe were calculated, with reference to Nagano and Tagawa [7], to be less than 1.8% and 2.3%, respectively.

2.2. Numerical method

The three-dimensional numerical simulations of the triple rectangular free jets for a small nozzle spacing of $S/d_e = 2.06$ ($S = 33$ mm) and a large nozzle spacing of $S/d_e = 4.13$ ($S = 66$ mm) were performed by OpenFOAM 5.0 using a finite volume method. The flow field was assumed to be unsteady, viscous, incompressible, isothermal, and fully turbulent. The unsteady flow simulation used the Implicit-LES turbulence model, where the Smagorinsky constant of the Smagorinsky-subgrid-scale (SGS) model was set to $C_s = 0$ [8]. The convection terms of the governing equations were discretized using the second-order unbounded central differencing scheme. The second-order central differencing scheme was used for the diffusion terms, while the second-order implicit scheme was used for the time marching. The pressure-implicit with splitting of operators (PISO) method was used as the calculation algorithm for the pressure-velocity coupling.

Figure 4 shows the computational domain, the mesh, and the boundary conditions for $S/d_e = 2.06$ and 4.13. Nonuniform spacing and structured meshes were used in the computational domain. The streamwise, vertical, and spanwise lengths of the computational domain are 640 mm ($= 40d_e$), 320 mm ($= 20d_e$), and 320 mm ($= 20d_e$), respectively. The width and the height of each nozzle are $C = 20$ mm

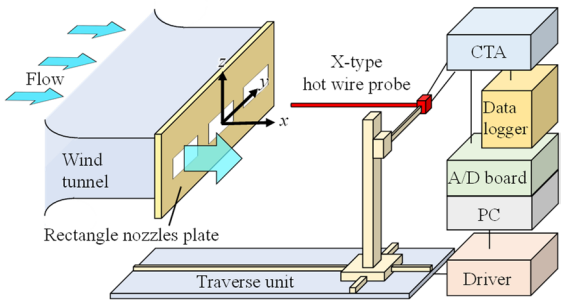

Figure 2. Schematic diagram of the experimental system.

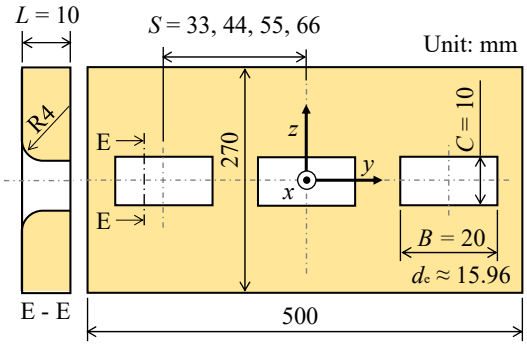

Figure 3. Schematic diagram of the orifice plate with triple rectangular nozzles.

and B = 10 mm, respectively. The effect of the number of grid points on the mean velocity profile was investigated for the triple rectangular jets with S/d_e =2.06. The numerical simulation was conducted with two numbers of grid points of approximately 1.3×10^7 and 6.5×10^6. The result for half the number of grid points deviated significantly from the experimental result. Therefore, the fine mesh was adopted for the numerical simulation, namely, the number of grid points was approximately 1.3×10^7 for S/d_e =2.06, and 1.8×10^7 for S/d_e = 4.13. The inlet boundary of the triple rectangular nozzles was set at a mean x-axial velocity of $\overline{u}$ = 14.2 m/s with x-direction velocity fluctuation of $u'_{rms}/\overline{u}$ = 0.02, the same as the experimental condition, and the gradient of zero was set for the pressure condition. The boundary condition of *pressureInletOutletVelocity* [9] was used at the top, bottom, outlet, and inlet surfaces of the computational domain. This boundary condition corresponds to a zero-gradient velocity everywhere on the boundary, except the inflow. When inflow occurred, a *fixedvalue* condition was applied to the tangential component. Furthermore, the pressure condition with the total pressure of 0 was set on each boundary of the computational domain. A time step size of 8×10^{-6} was used for the present simulation to satisfy the condition courant number CFL < 0.5.

3. RESILTS AND DISCUSSION

3.1. Comparison of experimental and numerical results

Figure 5 shows the profiles of the mean velocity $\overline{u}/\overline{u}_{0cl}$ along the x-axis in the x-y cross-section for nozzle spacing ratios of S/d_e = 2.06 and 4.13. The experimental profiles are in qualitative agreement with the simulation in both cases until the merging region. In particular, the agreement between the numerical simulations and the experimental results for S/d_e = 2.06 is good in the combined region of $x/d_e \geq 30$, and the agreement between the numerical simulations and the experimental results for S/d_e = 4.13 is also good at $x/d_e \geq 10$. In the following sections, the experimental results are discussed using the numerical simulation if necessary.

3.2. Mean velocity, and turbulent kinetic energy in the x-y cross section

Figure 6 shows contour plots of the mean x-axial velocity in the x-y cross-section, $\overline{u}/\overline{u}_{0cl}$, for triple rectangular free jets with S/d_e = 2.06, 4.13, and a single rectangular free jet of the SingleMajor case. The potential core region assumes a wedge shape due to the formation of the shear layer by mixing with the ambient fluid. The length of the potential core x_c is defined as the distance between the nozzle exit and

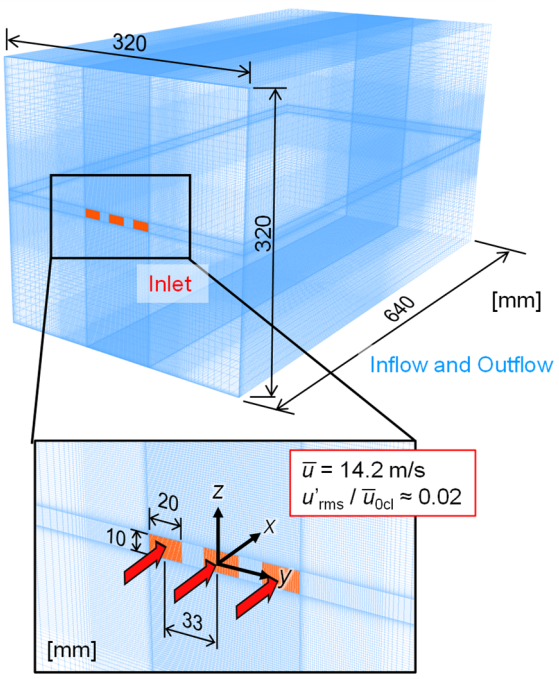

Figure 4. Computational domain, mesh and boundary conditions.

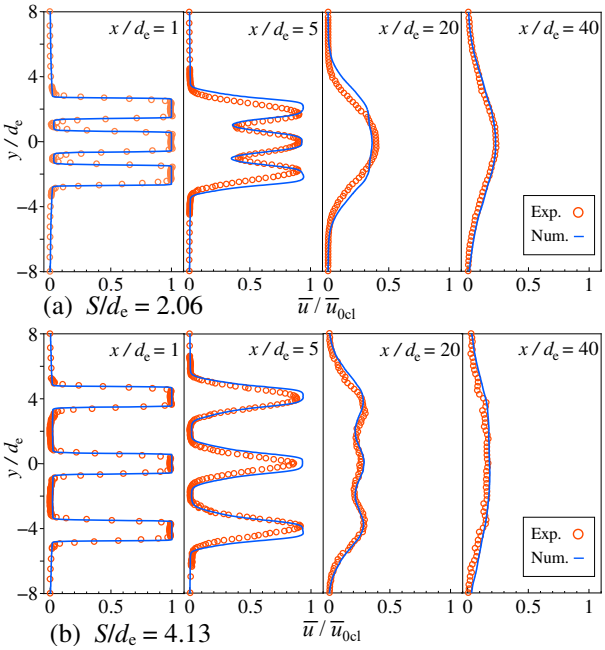

Figure 5. Profiles of mean velocity $\overline{u}/\overline{u}_{0cl}$ along x-axis in x-y cross section for (a) S/d_e = 2.06, and (b) S/d_e = 4.13 case.

the point at which $\overline{u}_{cl}/\overline{u}_{0cl}$ = 0.98 [2]. The length of the potential core of the rectangular jets is $x_c \approx 3d_e$ in all spacing ratios of triple rectangular jets and the SingleMajor case. The nozzle spacing has little effect on the length of the potential core. However, only for S/d_e = 2.06, it seems that the length of the wedge-shaped region of the middle jet becomes larger than that of the side jets. The middle jet does not cause the axis-switching phenomenon (discussed in Sec. 3.4). For a small spacing ratio S/d_e, the positions of the MP

and CP move upstream as compared with that for a large spacing ratio. In addition, the jet spread decreases in the downstream of CP due to the axis-switching phenomenon (discussed in Sec. 3.4). These results are consistent with those of Laban et al. [2], and Hayashida and Kiwata [4], who investigated the effect of nozzle spacing of twin round jets and twin rectangular free jets, respectively.

Figure 7 shows contour plots of the dimensionless turbulent kinetic energy in the x-y cross-section, $k/\overline{u}_{0cl}^2$ for triple rectangular free jets with $S/d_e = 2.06$, 4.13 and a single rectangular free jet of the SingleMajor case. At $0.5 \le x/d_e \le 5$, the turbulent kinetic energy increases in the inner and outer shear layers due to the Kelvin–Helmholtz instability. The y-direction position of the peak value of the turbulent kinetic energy of the side jets moves toward the middle jet. For $S/d_e = 2.06$, the turbulent kinetic energy ($k/\overline{u}_{0cl}^2 \ge 0.02$) in the outer shear layer of the side jets becomes larger than that in the outside inner shear layer of the side jets. At $5 \le x/d_e \le 10$, for a small spacing ratio of $S/d_e = 2.06$, the turbulent kinetic energy increases on the jet symmetry line because the larger mixing area in the middle jet does not expand in the x-direction. In the downstream region, the turbulent kinetic energy decreases gradually with the merging of the triple rectangular free jets. At $x/d_e \ge 20$, for $S/d_e = 2.06$, the turbulent kinetic energy increases more than that for the other spacing ratios due to the continuance of high velocity along the jet centerline as shown in Fig. 6. In contrast, the distribution of the turbulent kinetic energy of the triple rectangular free jets for $S/d_e = 4.13$ is not significantly different from that of the SingleMajor case. Thus, when the spacing ratio S/d_e is large, the flow characteristics of each jet in triple rectangular jets are similar to those of a single rectangular free jet.

3.3. Mean velocity and turbulent kinetic energy in the jet centerline and the jet symmetry line

Figure 8 shows the distributions of mean x-axial velocity on the middle jet centerline $\overline{u}_{cl,mid}/\overline{u}_{0cl}$, the side jets centerline $\overline{u}_{cl,side}/\overline{u}_{0cl}$, and the jet symmetry line $\overline{u}_{sym}/\overline{u}_{0cl}$. The results for twin rectangular jets with a spacing ratio of $S/d_e = 2.75$ [4], and the SingleMajor and the SingleRound cases are also shown in Fig. 8. the length of the potential cores, for the triple rectangular jets as described Sec. 3.2, and the TwinMajor and the SingleMajor jets are about $x_c \approx 3d_e$, respectively. This length of the potential core is smaller than that for the SingleRound case, that is, $x_c \approx 4d_e$. Commonly, the potential core length for a rectangular jet is shorter than that for a circular jet due to the three-dimensional deformation of the vortex rings in a non-circular jet [4]. From the end of the potential core region, the velocity on the jet centerline begins to decrease. The velocity on the jet centerline of a developed single circular jet and

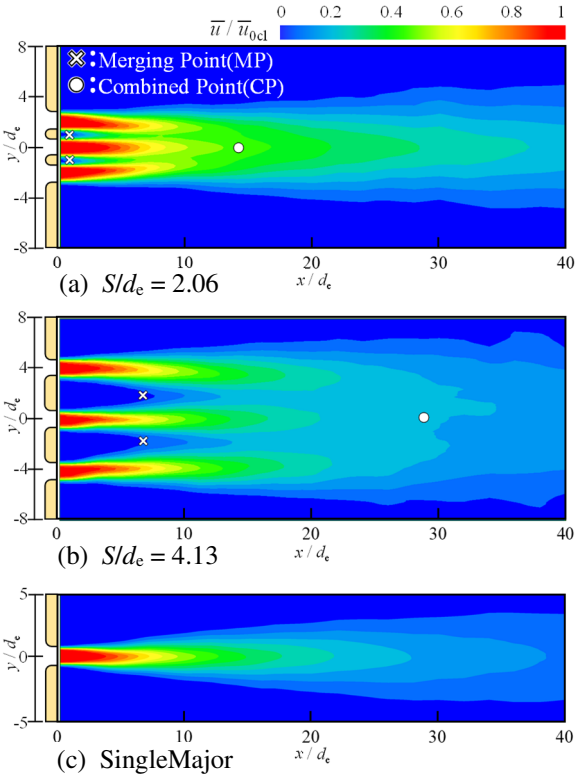

Figure 6. Contour plots of mean x-axial velocity in the x-y cross section for (a) $S/d_e = 2.06$, (b) $S/d_e = 4.13$ and (c) SingleMajor case.

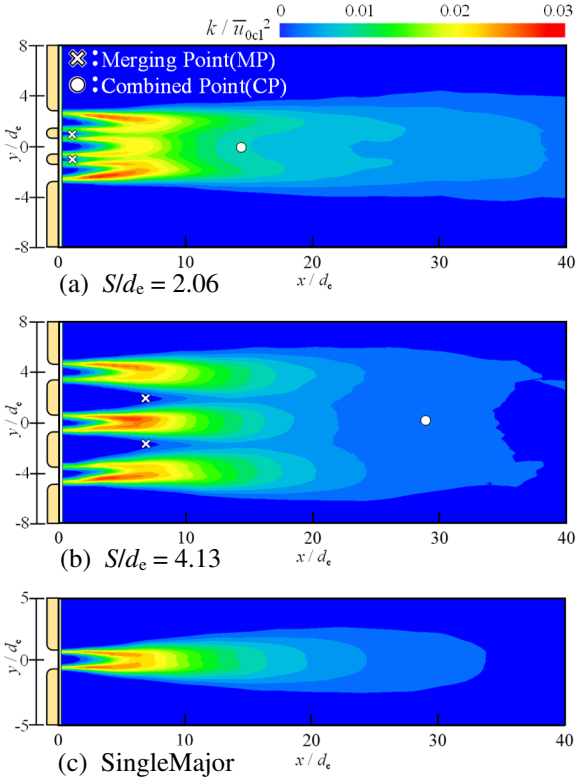

Figure 7. Contour plots of the turbulent kinetic energy in the x-y cross-section for (a) $S/d_e = 2.06$, (b) $S/d_e = 4.13$ and (c) SingleMajor case.

single rectangular jet, that is, SingleRound and SingleMajor, decays in proportion to x^{-1}. For S/d_e = 2.06, the velocity on the side jet centerline is lower than that on the middle jet centerline. However, for S/d_e = 4.13, the velocity on the side jet centerline is approximately the same as that on the middle jet centerline.

Figure 9 shows the second invariant iso-surfaces of the velocity gradient tensor Q from the numerical results for S/d_e = 2.06 and S/d_e = 4.13. For a small spacing ratio of S/d_e = 2.06, vortex rings at the nozzle exit are generated, and the middle and the side jets interfere between the outside and inside inner shear layers. From $x/d_e \approx 3$, longitudinal vortices are generated in the shear layer, and the vortices form a three-dimensional structure. As a result, the triple rectangular jets mix with the surrounding fluid, and a flow field develops. In contrast, for a large spacing ratio of S/d_e = 4.13, vortex rings at the nozzle exit are also generated. It seems that the interference between the outside and inside inner shear layers is weaker than that for a small spacing ratio of S/d_e = 2.06. The longitudinal vortex in the inner mixing region grows from about x/d_e = 5.

The distributions of the mean x-axial velocity, $\overline{u}_{sym}/\overline{u}_{0cl}$, on the jet symmetry line is also shown in Fig. 8. The MP, which is a point of the velocity deficit between the jets, is defined as the location where $\overline{u}_{sym} \approx 0.015\ \overline{u}_{0cl}$. The location of the MP is equal to $x/d_e \approx 1.1$, 2.8, 4.5, and 6.3 for S/d_e = 2.06, 2.75, 3.44, and 4.13, respectively. The location of the MP is close to the nozzle exit as the nozzle spacing ratio S/d_e decreases, similar to the case of the twin circular and twin rectangular jets [2, 4]. Downstream of the MP, the velocity of $\overline{u}_{sym}/\overline{u}_{0cl}$ on the jet symmetry line increases and has a peak value of 0.48, 0.3, 0.25, and 0.22 at $x/d_e \approx$ 9, 11, 15, and 17, respectively. Especially, for S/d_e = 2.06, the velocity $\overline{u}_{sym}/\overline{u}_{0cl}$ exhibits a high rate of increase because of the mixing between the middle and the side jets with the axis-switching phenomenon similar to that of the twin rectangular free jets [4].

The CP is defined as the location where $\overline{u}_{cl} \approx \overline{u}_{sym}$. The CP moves upstream with the decreasing nozzle spacing ratios, that is, $x/d_e \approx$ 14, 19, 24, and 29 for S/d_e = 2.06, 2.75, 3.44, and 4.13, respectively. The location of the CP is approximately proportional to the nozzle spacing ratio S/d_e, similar to the case of twin circular jets and twin rectangular jets [2, 4]. Downstream of the CP, the velocity $\overline{u}_{cl,mid}/\overline{u}_{0cl}$ on the jet centerline for a small spacing ratio of S/d_e = 2.06 is larger than that for a large spacing ratio S/d_e = 4.13. At x/d_e = 40, the velocity $\overline{u}_{cl,mid}/\overline{u}_{0cl}$ on the jet centerline for triple rectangular free jets of S/d_e =

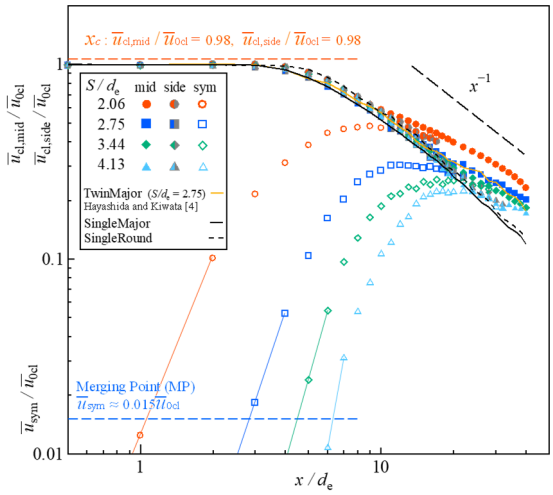

Figure 8. Distributions of the mean x-axial velocity on the jet centerline and the jet symmetry line along the x-axis.

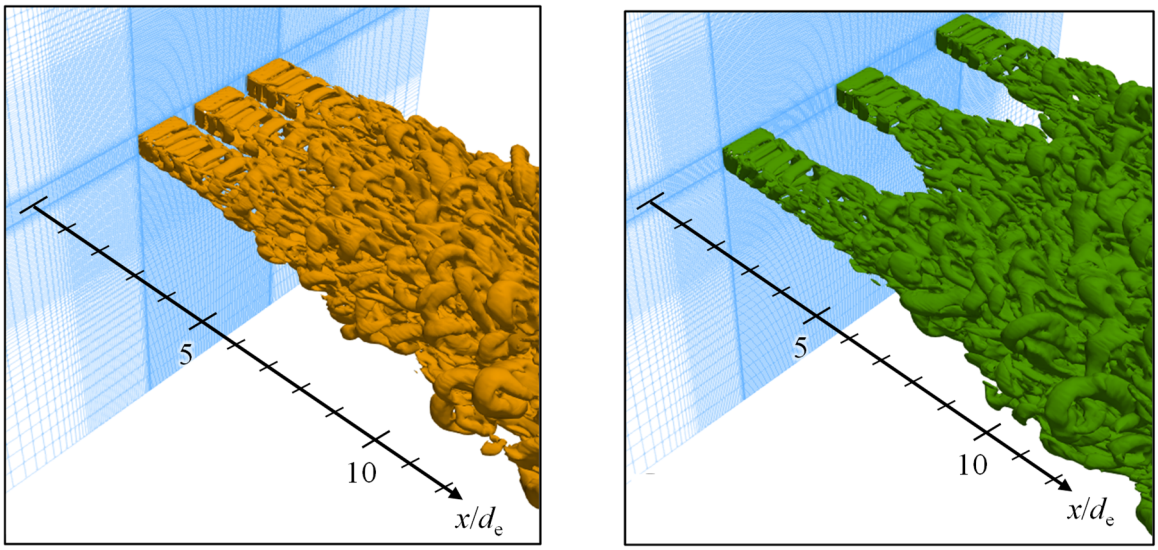

(a) S/d_e = 2.06 (b) S/d_e = 4.13

Figure 9. Second invariant iso-surfaces of the velocity gradient tensor Q for (a) S/d_e = 2.06 and (b) S/d_e = 4.13

2.75 is larger than that for twin rectangular free jets with the same spacing ratio. However, because the values are nearly identical at $x/d_e \leq 30$, the decrease in velocity of the twin rectangular jets at $x/d_e = 40$ is considered to be due to a difference in the flow rate of the jets.

3.4. Mean velocity in the y-z cross-section

Figure 10 shows contour plots of the mean x-axial velocity, $\overline{u}/\overline{u}_{0cl}$, in the y-z cross-section at x/d_e = 1, 5, 10, 20, 30, and 40 for triple rectangular free jets with S/d_e = 2.06, 2.75, and 4.13.

For S/d_e = 2.06, the cross-sectional shape of the side jets at x/d_e = 1 changes only at the corners on the side of the outer mixing region. Namely, these shapes change from rectangular to trapezoidal. From x/d_e = 5, the jets begin to merge. At x/d_e = 10, the triple rectangular free jets merge and form a horizontally long elliptic cross-sectional shape. At x/d_e = 20, the cross-section of merged triple rectangular free jets becomes round. At x/d_e = 40, this cross-section in the downstream region has a vertically long elliptic cross-sectional shape and retains a large area of mean velocity of $\overline{u}/\overline{u}_{0cl}$ = 0.18. Thus, the triple rectangular free jets for a small nozzle spacing ratio in the downstream exhibit an axis-switching phenomenon after jet merger. Specifically, at x/d_e < 5 for S/d_e = 2.06, the cross-sectional shape of the middle jet has a small elongation in the z-direction compared to the side jets, and the major axis of the cross-sectional shape is oriented in the y-direction. Thus, triple rectangular jets with a small nozzle spacing ratio may suppress the axis-switching phenomenon of the middle jet due to interference with the side jets.

For S/d_e = 2.75, the mixing development process for triple rectangular free jets shows a middle process between S/d_e = 2.06 and 4.13.

For S/d_e = 4.13 at x/d_e = 1, the cross-section of jets begins to deform, and the four corners of each rectangular jet each become round, that is, the axis-switching phenomenon starts. From x/d_e = 10, the merging of the whole jets begins. At x/d_e = 30, the merged jets have a horizontally long elliptic cross-sectional shape.

Downstream at x/d_e = 30 for S/d_e = 2.06 and 4.13, the contour plots of the velocity of the secondary flow and the velocity vector maps obtained from the numerical simulations are shown in Fig. 11. For S/d_e = 2.06, the vortices were generated on the four sides of the combined jet as they rolled up along the z-direction, suggesting that the axis-switching phenomenon occurred from x/d_e = 20 to 40 as shown in Fig. 10(a). In contrast, for S/d_e = 4.13, there was no roll-up to the z-direction, and the combined jet uniformly spread in the y- and z-directions.

5. CONCLUSIONS

The influence of nozzle spacing on the flow characteristics of triple rectangular jets with an aspect ratio of 2 was experimentally and numerically investigated at a Reynolds number of Re = 15,000. The results are summarized as follows:

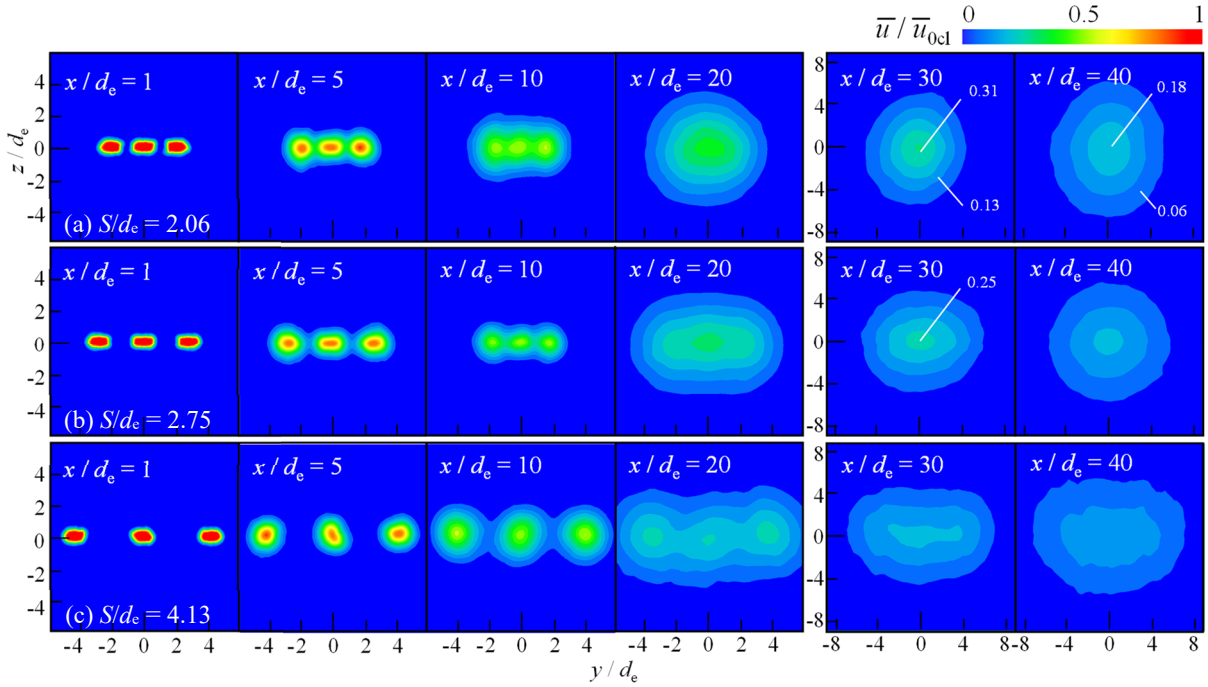

Figure 10. Contour plots of streamwise mean velocity in the y-z cross section for (a) S/d_e = 2.06, (b) S/d_e = 2.75, and (c) S/d_e = 4.13 case.

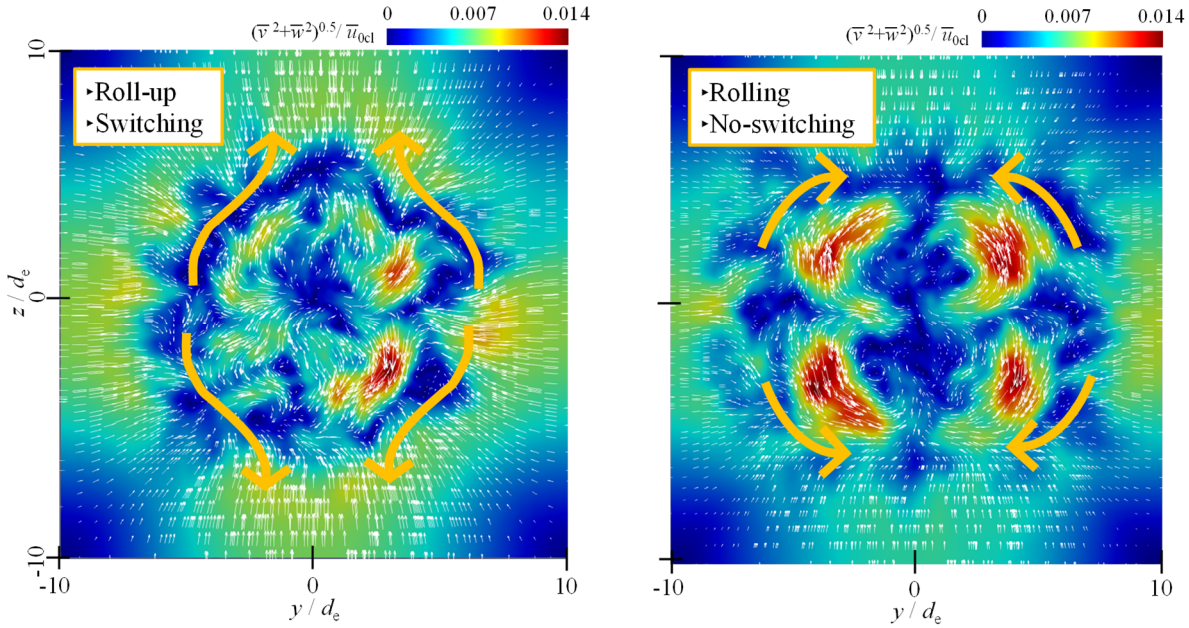

(a) $S/d_e = 2.06$ (b) $S/d_e = 4.13$

Figure 11. Contour plots of secondary flow and vector maps from numerical results at $x/d_e = 30$ for (a) $S/d_e = 2.06$, and (b) $S/d_e = 4.13$ case.

(1) For a small nozzle spacing ratio $S/d_e = 2.06$, the MP and CP move upstream, the mean velocity and turbulent kinetic energy increase on the jet symmetry line, and these increase on the jet centerline after the CP. Therefore, the triple rectangular jets with a small spacing ratio have a large mixing between the middle and side jets from upstream.

(2) For large nozzle spacing ratio, that is, $S/d_e = 4.13$, before the jets merge, the flow characteristics of the triple rectangular free jets were similar to that of the single rectangular free jet.

REFERENCES

[1] Okamoto, T., Yagita, M., Watanabe, A. and Kawamura, K., Interaction of twin circular jet, *Bulletin of JSME*, Vol. 28, No. 238(1985), pp. 617-622.

[2] Laban, A., Aleyasin, S. S., Tachie, M. F. and Koupriyanov, M., Experimental investigation of nozzle spacing effects on characteristics of round twin free jets, *Journal of Fluids Engineering*, Vol.141, No.7 (2019), pp.1-11.

[3] Aleyasin, S. S. and Tachie, M. F., Statistical properties and structural analysis of three-dimensional twin round jets due to variation in Reynolds number, *International Journal of Heat and Fluid Flow*, Vol.76 (2019), pp. 215-230.

[4] Hayashida, K. and Kiwata, T., Effects of nozzle orientation and spacing on flow characteristics of twin rectangular jets, *Transactions of the JSME*, Vol.89, No.927 (2023), Paper No.23-00193, pp.1-18 (in Japanese).

[5] Morris, E. M., Aleyasin, S. S. Biswas, N., and Tachie, M. F., Turbulent properties of triple elliptic free jets with various nozzle orientation, *Journal of Fluids Engineering*, Vol.142, No.3 (2020), pp.1-13.

[6] Teramoto, H., Kiwata, T. and Yajima, K., Influence of nozzle aspect ratio and orientation on flow characteristics of multiple elliptic jets, *Journal of Fluid Science and Technology*, Vol.15, No.2 (2020), Paper No.19-00579.

[7] Nagano, Y. and Tagawa, M., An error analysis of hot-wire measurements, Transactions of the *Japan Society of Mechanical Engineers*, Series B, Vol.54, No.503 (1988), pp.1642-1648 (in Japanese).

[8] Matsuyama, C., OK, LES. tell me the answer for turbulent planar jet, *Proceedings of Fluid Dynamics Conference / Aerospace Numerical Simulation Symposium 2020* (online) (2020), pp.83-91 (in Japanese).

[9] OpenCFD Ltd., OpenFOAM User Guide ver.12 (2024), pp. U-43.

[10] Harima, T., Fujita, S. and Osaka, H., Mixing and diffusion processes of twin circular free jets with various nozzle spacing, Proceedings of the JSME Annual Meeting' 2000 (2000), Paper No.1912 (in Japanese)